SPE 163609

A Generalized Framework Model for Simulation of Gas Production in Unconventional Gas Reservoirs

Yu-Shu Wu, SPE, Colorado School of Mines, Jianfang Li, SPE, RIPED of PetroChina, Didier Ding, SPE, IFPEN, Cong Wang, SPE, Colorado School of Mines, and Yuan Di, Peking University

This paper was prepared for presentation at the SPE Reservoir Simulation Symposium held in The Woodlands, Texas USA, 18–20 February 2013.

Abstract

Unconventional gas resources from tight sand and shale gas reservoirs have received great attention in the past decade around the world, because of their large reserves as well as technical advances in developing these resources. As a result of improved horizontal drilling and hydraulic fracturing technologies, the progresses are being made towards commercial gas production from such reservoirs, as demonstrated in the US. However, understandings and technologies needed for effective development of unconventional reservoirs are far behind the industry needs, e.g., gas recovery rates from those unconventional resources remain very low. There are some efforts in the literature on how to model gas flow in shale gas reservoirs using various approaches from modified commercial simulators to simplified analytical solutions, leading to limited success. Compared with conventional reservoirs, gas flow in ultra-low permeability unconventional reservoirs is subject to more nonlinear, coupled processes, including nonlinear adsorption/desorption, non-Darcy flow (at high flow rate and low flow rate), and strong rock-fluid interaction, and rock deformation within nano-pores or micro-fractures, coexisting with complex flow geometry and multi-scaled heterogeneity. Therefore, quantifying flow in unconventional gas reservoirs has been a significant challenge and traditional REV-based Darcy law, for example, may not be in general applicable.

In this paper, we will discuss a generalized mathematical model and numerical approach for unconventional gas reservoir simulation. We will present a unified framework model able to incorporate all known mechanisms and processes for two-phase gas flow and transport in shale gas or tight gas formations. The model and numerical scheme are based on generalized flow models using unstructured grids. We will discuss the numerical implementation of the mathematical model and show results of our model verification effort. Specifically, we discuss a multi-domain, multi-continuum concept for handling multi-scaled heterogeneity and fractures, i.e., using hybrid modeling approaches to describe different types and scales of fractures from explicitly modeling of hydraulic fractures and fracture network in simulated reservoir volume (SRV) to distributed naturally fractures, microfractures, and tight matrix. We will demonstrate model application to quantify hydraulic fractures and transient flow behavior in shale gas reservoirs.

Introduction

Even with the significant progress made in producing natural gas from unconventional, low-permeability shale gas and tight gas reservoirs in the past decade, gas recovery remains very low (estimated at 10-30% of GIP). Gas production or flow in such extremely low-permeability formations is further complicated by many co-existing processes, such as severe heterogeneity, large Klinkenberg effect (Klinkenberg, 1941), nonlinear or non-Darcy flow behavior, adsorption/desorption, strong interactions between fluids (gas and water) molecules and solid materials within tiny pores, as well as micro- and macro-fractures of shale and tight formations. Currently, there is little in basic understanding on how these complicated flow behavior impacts on gas flow and the ultimate gas recovery in such reservoirs. In particular, there are few effective reservoir simulators currently available or few modeling studies (e.g., Kelkar and Atiq, 2010) in the industry for assisting reservoir engineers to model and develop the unconventional natural gas resources.

Shale formation is characterized by extremely low permeability from subnanodarcys to microdarcys and is different for different type of shales, even under the similar porosity, stress, or pore pressure. As summarized by Wang et al. (2009), the permeability of deep organic-lean mudrocks ranges from smaller than to tens of nanodarcys, while permeability values in

organic-rich gas shales from subnanodarcys to tens of microdarcys. The Klinkenberg effect (Klinkenberg, 1941) has been practically ignored in conventional gas reservoir studies, except in some cases when analyzing pressure responses or flow near gas production wells at very low pressure. This is because of larger pore size and relatively high pressure existing in those conventional gas reservoirs. In shale gas reservoirs, however, the Klinkenberg or slippage effect is expected to be significant, because of the nano-size pores of such rock, even under high pressure condition. Wang et al. (2009) show that gas permeability in the Marcellus Shale increases from 19.6 μD at 1,000 psi to 54 μD at 80 psi, because of the strong slippage effect.

Unconventional reservoir dynamics is characterized by highly nonlinear behavior of multiphase flow in extremely low-permeability rock, coupled by many co-existing physical processes, e.g., non-Darcy flow. Because of complicated flow behavior, strong interaction between fluid and rock as well as multi-scaled heterogeneity, the traditional Darcy-law-and-REV-based model may not be in general applicable for describing flow phenomena in unconventional gas reservoirs. Blasingame (2008) and Moridis et al. (2010) provide very comprehensive review of flow mechanisms in unconventional shale gas reservoirs. Both studies point out that non-laminar/non-Darcy flow concept of high-velocity may turn out to be important in shale gas production. The non-laminar/non-Darcy flow concept of high-velocity flow of gas flow in shale gas reservoirs may not be represented by Darcy's law and the *Forchheimer* equation is probably sufficient for many applications.

Natural gas in shale gas formations is present both as a free gas phase and as adsorbed gas on solids in pores. In these reservoirs, gas or methane molecules are adsorbed mainly to the carbon-rich components, i.e. kerogen (Silin and Kneafsey, 2011; Mengal and Wattenbarger, 2011; EIA, 2011). The adsorbed gas represents significant quantities of total gas reserves (20-80%) as well as recovery rates, which cannot be ignored in any model or modeling analysis. In shale gas formations, the past studies have found that methane molecules are adsorbed mainly to the carbon-rich components, i.e. kerogen, correlated with total organic content (TOC) in shales, as a function of reservoir pressure.

In conventional oil or gas reservoirs, effect of geomechanics on rock deformation and permeability is generally small and has been mostly ignored in practice. However, in unconventional shale formations with nano-size pores or nano-size microfractures, such geomechanics effect can be relatively large and may have a significant impact on both fracture and matrix permeability, which has to be considered in general. Wang et al. (2009) show that permeability in the Marcellus Shale is pressure dependent and decreases with an increase in confining of pore pressure (or total stress). The effect of confining pressure on permeability is caused by a reduction of porosity. Bustin et al. (2008) report the effect of stress (confining pressure) in Barnett, Muskwa, Ohio, and Woodford shales and show that degree of permeability reduction with confining pressure is significantly higher in shales than that in consolidated sandstone or carbonate.

This paper presents a generalized mathematical model and numerical approach for unconventional gas reservoir simulation. We will present a unified framework model that is able to incorporate all known mechanisms and processes for two-phase gas flow in shale gas or tight gas formations. The numerical scheme is based on generalized flow models using unstructured grids. We will discuss the numerical implementation of Klinkenberg effects, non-Darcy flow, gas adsorption and geomechanics effects into the mathematical model. Results of our model verification effort will be also presented. We will demonstrate model application to quantify hydraulic fractures and transient flow behavior in shale gas reservoirs.

One of the critical issues in shale gas reservoir simulation is how to handle fracture flow and interaction. This is because the gas flow and production relies on fractures in these reservoirs. Cipolla et al. (2009) built a methodology on modeling complex fracture geometry and heterogeneity from the micro-seismic data. In this paper, we present a hybrid-fracture modeling approach, defined as a combination of explicit-fracture, multi-continuum, MINC (Pruess and Narasimham, 1985), and single-porosity modeling approaches, which seems the best option for modeling a shale gas reservoir with both hydraulic fractures and natural fractures. This is because hydraulic fractures, which have to be dealt with for shale gas production, are better handled by the explicit fracture method but cannot be modeled in general by a dual-continuum model. On the other hand, natural fractured reservoirs are better modeled by a dual-continuum approach, such as MINC for extremely low-permeability matrix in shale gas formations, which cannot be modeled by an explicit fracture model. Specifically, we demonstrate how to use the hybrid modeling approach to describe different types and scales of fractures from explicitly modeling of hydraulic fractures and fracture network in simulated reservoir volume (SRV) to distributed naturally fractures, microfractures, and tight matrix.

Flow Governing Equations

In most cases of gas production from shale gas formations, a two-phase, gas-liquid flow model or a multi-phase flow model is considered to be sufficient for simulation studies. This is because what we are most concerned with in shale gas reservoir simulation is to model gas flow from reservoir to well. However, in addition to gas phase, liquid phase flow is often occurring simultaneously with gas flow, needed to be considered in the following cases: (1) there exists of mobile *in-situ* connate water; (2) there exist a lot of aqueous hydraulic fracturing fluids, which are sucked into the formations surrounding wells; and (3) there may exist large amount of gas condensate inside reservoir under *in-situ* pressure and temperature condition during

production. Therefore, in this paper we primarily discuss two-phase (gas and liquid) flow model and formulation and treat single-phase gas flow as a special case of the two-phase flow for simulation studies of unconventional gas reservoirs.

A multiphase system of gas and water (or liquid) in a porous or fractured unconventional reservoir is assumed to be similar to what is described in a black oil model, composed of two phases: gaseous and aqueous phases. For simplicity, the gas and water components are assumed to be present only in their associated phases and adsorbed gas is within the solid phase of rock. Each fluid phase flows in response to pressure, gravitational, and capillary forces according to the multiphase extension of Darcy law or several extended non-Darcy flow laws, discussed below. In an isothermal system containing two mass components, subject to multiphase flow and adsorption, two mass-balance equations are needed to fully describe the system, as described in an arbitrary flow region of a porous or fractured domain for flow of phase β (β = g for gas and β = w for water),

$$\frac{\partial}{\partial t}(\phi S_\beta \rho_\beta + m_g) = -\nabla \bullet (\rho_\beta \mathbf{v}_\beta) + q_\beta \tag{1}$$

where ϕ is the effective porosity of porous or fractured media; S_β is the saturation of fluid β; ρ_β is the density of fluid β; $\mathbf{v}_\beta$ is the volumetric velocity vector of fluid β, determined by Darcy's law or non-Darcy's flow models, discussed in the below; t is time; m_g is the adsorption or desorption mass term for gas component per unit volume of formation; and q_β is the sink/source term of phase (component) β per unit volume of formation,

Incorporation of Gas Adsorption and Desorption: The amount of adsorbed gas in a given shale gas formation is generally described using the Langmuir's isotherm (e.g., Mengal and Wattenbarger, 2011; Silin and Kneafsey, 2011; EIA, 2011; Moridis et al. 2010; Wu et al. 2012), i.e., it is correlated to reservoir gas pressure. To incorporate the gas adsorption or desorption mass term in the mass conservation equation, the amount of adsorbed gas is determined according to the Langmuir's isotherm as a function of reservoir pressure. As the pressure decreases with continuous gas production through production wells in reservoirs, more adsorbed gas is released from solid to free gas phase in the pressure lowering region, contributing to the total gas flow or production. In our model, the mass of adsorbed gas in unit formation volume is described (Leahy-Dios et al. 2011; Wu et al. 2012):

$$m_g = \rho_R \rho_g V_E \tag{2}$$

where m_g is absorbed gas mass in unit formation volume; ρ_R is rock bulk density; ρ_g is gas density at standard condition; V_E is the adsorption isotherm function or gas content in scf/ton (or standard gas volume adsorbed per unit rock mass). If the adsorbed gas terms can be represented by the Langmuir isotherm (Langmuir, 1916), the dependency of adsorbed gas volume on pressure at constant temperature is given below,

$$V_E = V_L \frac{P}{P + P_L} \tag{3}$$

where V_L is the Langmuir's volume in scf/ton; P is reservoir gas pressure; and P_L is Langmuir's pressure, the pressure at which 50% of the gas is desorbed. In general, Langmuir's volume. V_L is a function of the organic richness (or TOC) and thermal maturity of the shale and one example for gas adsorbed curve is illustrated in **Figure 1** for the Marcellus Shale (EIA, 2011).

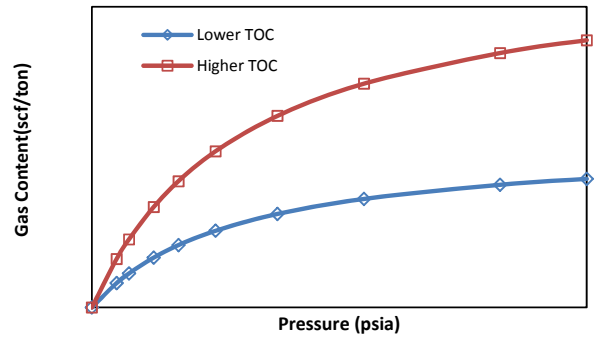

Figure 1 Marcellus Shale Adsorbed Gas Content (EIA, 2011)

Note that Equation (3) is valid only for the case when the Langmuir model is applicable. In general, V_E in Equation (2) can be determined from any correlation of gas adsorption as a function of reservoir gas pressure, which may be defined by a table lookup, from laboratory studies, for a given unconventional reservoir.

In the literature, the most commonly used empirical model describing sorption onto organic carbon in shales is analogous to that used in coal bed methane and follows the Langmuir isotherm (Gao et al. 1994; Moridis et al. 2010), such as Equations (2) and (3). This adsorption modeling approach is based on the assumption that an instantaneous equilibrium exists between the sorbed and the free gas, i.e., here is no transient-time lag between pressure changes and the corresponding sorption/desorption responses, i.e., the equilibrium model of the Langmuir sorption is assumed to be valid, which provides generally good approximation in shale gas modeling. Several kinetic sorption models exists in the literature using diffusion approaches, however, the subject has not been fully investigated or understood (Moridis et al. 2010).

Coupled Flow and Geomechanics Effect: In this section, we will propose a very practical modeling approach, easily to implement to an existing reservoir simulator, to couple geomechanics with two-phase flow in unconventional reservoirs. The following discussion is based on our previous work (e.g., Wu et al. 2008; Winterfeld and Wu, 2011). The effective porosity, permeability, and capillary pressure of rock are assumed to correlate with the mean effective stress (σ'_m), defined as,

$$\sigma'_m = \sigma_m(x, y, z, P) - \alpha P \tag{4}$$

where α is the Biot constant and

$$\sigma_m(x,y,z,P)=(\sigma_x(x,y,z,P)+\sigma_y(x,y,z,P)+\sigma_z(x,y,z,P))/3 \tag{5}$$

where σ_x, σ_y, and σ_z are total stress in x, y, and z- directions, respectively. With the definition of the mean effective stress in Equation (5), the effective porosity of formation (fractures or porous media) is defined as a function of mean effective stress only,

$$\phi = \phi\left(\sigma'_m\right) \tag{6}$$

Similarly, the intrinsic permeability is related to the effective stress, i.e.,

$$k = k\left(\sigma'_m\right) \tag{7}$$

For capillary-pressure functions, the impact of rock-deformation or pore-change is accounted for using the Leverett function (Leverett, 1941),

$$P_c = C_p P_c^0\left(S_w\right)\frac{\sqrt{k^0/\phi^0}}{\sqrt{k(\sigma'_m)/\phi(\sigma'_m)}} \tag{8}$$

where P_c is the capillary pressure between gas and water as a function of water or gas saturation; C_p is a constant; and the superscript 0 denotes reference or zero-stress condition.

Several correlations have been used for porosity as a function of effective stress and permeability as a function of porosity (Davies and Davies, 1999, Rutqvist et al. 2002, Winterfeld and Wu, 2011 and 2012). In our numerical implementation, the function for porosity and permeability presented by Rutqvist et al. (2002) is adopted, which is obtained from laboratory experiments on sedimentary rock (Davies and Davies, 1999),

$$\phi = \phi_r + (\phi_0 - \phi_r)e^{-a\sigma'} \tag{9}$$

where ϕ_0 is zero effective stress porosity; ϕ_r is high effective stress porosity; and the exponent a is a parameter. They also present an associated function for permeability in terms of porosity,

$$k = k_o e^{c\left(\frac{\phi}{\phi_0} - 1\right)} \tag{10}$$

where c is a parameter. **Figure 2** shows effect of confining pressure on gas permeability in gas shales.

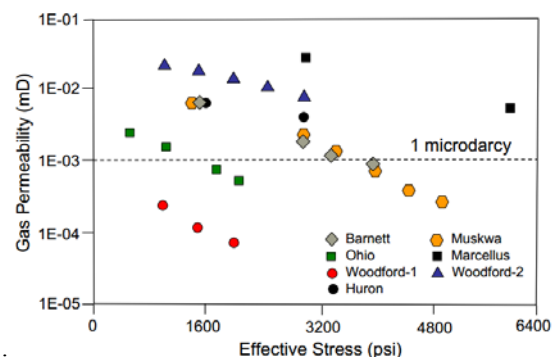

Figure 2 Effect of confining pressure on gas permeability in gas shales. (Wang et al. 2009)

An alternative table lookup approach is given for the correlation of reservoir porosity and permeability as a function of effective mean stress, from laboratory studies, for a given unconventional reservoir.

It has to be mentioned that Figure 2 from Wang et al. (2009) presents the permeability measurement from core plugs where potential natural microfractures in core plugs play an important role for the connectivity. If crushed samples are used to measure the matrix permeability only by eliminating natural and drilling induced microfactures, the permeability value is one or two orders lower. The geomechanics has a much stronger impact on the fracture than on the matrix. So, when using a dual-porosity approach in the modeling, if microfractures are considered as a part of the matrix media, the above relations can be directly applied. However, if microfractures are considered as a part of the fractured media, the geomechanics effect is more complex because fracture conductivities are subjected to different laws according to microfractures, partially propped fractures or propped fractures (Cipolla et al. 2009).

The applicability of these mechanics coupling models in multiphase flow simulations for rock deformation effect requires that the initial distribution of effective stress or total stress field be predetermined as a function of spatial coordinates and pressure fields, as in Equation (5). In practice, the stress distribution may be estimated analytically, numerically, or from field measurements, because changes in effective stress are primarily caused by changes in reservoir pressure during production. These models can be significantly simplified for coupling multiphase gas flow with rock deformation in stress-sensitive formations in numerical simulation, if the *in situ* total stress in reservoirs is constant or a function of spatial coordinates as well as fluid pressure only.

Incorporation of Klinkenberg or Gas Slippage Effect: In low-permeability shale gas formations with nano-size pores or under low reservoir pressure condition, Klinkenberg effect (Klinkenberg, 1941) may be significant and should be accounted for when modeling gas flow in such reservoirs (Wang et al. 2009; Wu et al. 1998). As discussed above, Klinkenberg effect is

expected to be larger or stronger in unconventional reservoirs, because of small pore size and low permeability associated, in comparison with that in conventional reservoirs. Klinkenberg effect, if existing, will enhance gas permeability or productivity in a low-pressure zone, such as the region near a well, of low-permeability unconventional formations and therefore should be included as an additional beneficial factor of gas flow enhancement.

Klinkenberg effect is incorporated in gas flow models by modifying absolute permeability for the gas phase as a function of gas pressure (e.g., Wu et al. 1998),

$$k_g = k_\infty \left(1 + \frac{b}{P_g}\right) \tag{11}$$

where k_∞ is constant, absolute gas-phase permeability under very large gas-phase pressure (where the Klinkenberg effect is minimized); and b is the Klinkenberg b-factor and could be pressure or temperature dependent, accounting for gas-slippage effect.

In conventional gas reservoir simulation, the b-factor is commonly treated as constant and determined depending on the pore structure of the medium and formation temperature for a particular reservoir. Several recent studies on dynamic gas slippage using micro-scale or pore-scale models have considered the b-factor as a function of gas pressure or Knudsen number. In application, the Klinkenberg effect should be modeled using laboratory-determined b-factor either as constant or as a pressure-dependent function. An example relation between permeability and pressure, as shown in **Figure 3**, can be directly used for the reservoirs concerned, if site-specific study provides such correlations or plots.

Comparing **Figure 2** and **Figure 3**, it seems that the Klinkenberg effect has much less impact than that of geomechanics, and they are in the opposite directions. But they are not applied to the same media. Geomechanics has an effect on the microfractures and drilling induced fractures, while the Klinkenberg effect is applied on the matrix media only.

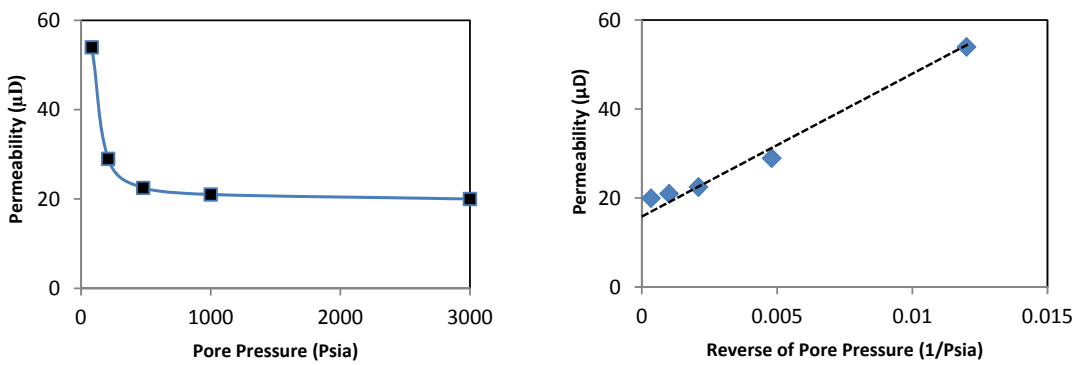

Figure 3 Effect of pore pressure on gas permeability in the Marcellus Shale, with a confining pressure of 3,000 psi (Soeder, 1988; Wang et al. 2009)

Incorporation of non-Darcy Gas Flow: In addition to multiphase Darcy flow, non-Darcy flow may also occur between and among the continua, such as along fractures, in unconventional gas reservoirs. The flow velocity, $\mathbf{v}_\beta$, for non-Darcy flow of each fluid may be described using the multiphase extension of the *Forchheimer* equation (e.g., Wu, 2002),

$$-\left(\nabla \Phi_\beta\right) = \frac{\mu_\beta}{k_{r\beta}} k\, \mathbf{v}_\beta + \beta_\beta \rho_\beta \mathbf{v}_\beta \left|\mathbf{v}_\beta\right| \tag{12}$$

where β_β is the effective non-Darcy flow coefficient with a unit m^{-1} for fluid β under multiphase flow conditions. The non-Darcy flow correlation from Tek et al. (1962) may be used to evaluate the non-Darcy flow coefficient β_β versus porosity and permeability as follows:

$$\beta_\beta = \frac{C_\beta}{k^{5/4}\phi^{3/4}} \tag{13}$$

Non-Darcy Flow at Low Flow Rates: The phenomenon of flow with threshold-pressure-gradient concept has been observed in laboratory and is commonly used to describe nonlinear flow behavior in low permeability reservoirs (Xiong et al. 2008; Lei et al. 2007). This flow condition is similar to Binghan non-Newtonian flow through porous media, which is used in this work to describe conditions where flow may not occur until the pressure or potential gradient reaches a certain threshold value (Wu and Pruess, 1998). Instead of introducing an apparent viscosity for Bingham fluid, an effective potential gradient approach, as follows, has been proven to be more efficient numerically (Wu et al., 1992). Using the effective potential gradient, the flow of gas or liquid in a low-permeability reservoir is described by,

$$\mathbf{v}_\beta = -\frac{k\, k_{r\beta}}{\mu_b}\left(\nabla\Phi_e^\beta\right) \tag{14}$$

where μ_b is the Bingham plastic viscosity coefficient for phaseβ; and $\nabla\Phi_e^\beta$ is the effective potential gradient whose scalar component in the x direction (the flow direction) is defined as,

$$\left(\nabla\Phi_e\right)_x = \left(\nabla\Phi\right)_x - G \quad \text{for} \quad \left(\nabla\Phi\right)_x > G \tag{15}$$

$$\left(\nabla\Phi_e\right)_x = \left(\nabla\Phi\right)_x + G \quad \text{for} \quad \left(\nabla\Phi\right)_x < -G \tag{16}$$

$$\left(\nabla\Phi_e\right)_x = 0 \quad \text{for} \quad -G < \left(\nabla\Phi\right)_x < G \tag{17}$$

Numerical Model

As discussed above, the PDE that governs gas and liquid flow in shale gas reservoirs is nonlinear. In addition, gas flow in unconventional reservoirs is subject to many other nonlinear flow processes, such as adsorption and non-Darcy flow. In general, the flow model needs to be solved using a numerical approach. This work follows the methodology for reservoir simulation, i.e., using numerical approaches to simulate gas and water flow, following three steps: (1) spatial discretization of mass conservation equations; (2) time discretization; and (3) iterative approaches to solve the resulting nonlinear, discrete algebraic equations.

Discrete Equations: The component mass-balance Equations (Equation (1)) are discretized in space using a control-volume or integrated finite difference concept (Pruess et. at. 1999). The control-volume approach provides a general spatial discretization scheme that can represent a one-, two- or three-dimensional domain using a set of discrete meshes. Each mesh has a certain control volume for a proper averaging or interpolation of flow and transport properties or thermodynamic variables. Time discretization is carried out using a backward, first-order, fully implicit finite-difference scheme. The discrete nonlinear equations for components of gas and water at gridblock or node i can be written in a general form:

$$\left\{(\phi\rho S)_i^{\beta,n+1} + m_i^{\beta,n+1} - (\phi\rho S)_i^{\beta,n} - m_i^{\beta,n}\right\}\frac{V_i}{\Delta t} = \sum_{j\in\eta_i} \text{flow}_{ij}^{\beta,n+1} + Q_i^{\beta,n+1} \tag{18}$$

(β = gas and liquid) and (i=1, 2, 3, …, N)

where superscript β serves also as an equation index for gas and water components with β = 1 (gas) and 2 (water); superscript n denotes the previous time level, with n+1 the current time level to be solved; subscript i refers to the index of gridblock or node i, with N being the total number of nodes in the grid; Δt is time step size; V_i is the volume of node i; η_i contains the set of direct neighboring nodes (j) of node i; m_i^k, flow_{ij}^k, and Q_i^k are the absorption or desorption, the component mass "flow" term between nodes i and j, and sink/source term at node i for component k, respectively.

The "flow" terms in Equation. (18) are mass fluxes by advective processes and are described, when Darcy's law is applicable, by a discrete version of Darcy's law, i.e., the mass flux of fluid phase β along the connection is given by

$$\text{flow}_{ij}^{\beta} = \lambda_{\beta,ij+1/2}\gamma_{ij}\left(\Phi_{\beta j} - \Phi_{\beta i}\right) \tag{19}$$

where $\lambda_{\beta,i\,j+1/2}$ is the mobility term to phase β, defined as

$$\lambda_{\beta,i\,j+1/2} = \left(\frac{\rho_\beta k_{r\beta}}{\mu_\beta}\right)_{ij+1/2} \tag{20}$$

In Equation (19), γ_{ij} is transmissivity and is defined, for a Voronoi grid, as (Pruess et al. 1999),

$$\gamma_{ij} = \frac{A_{ij}k_{ij+1/2}}{D_i + D_j} \tag{21}$$

where A_{ij} is the common interface area between the connected blocks or nodes i and j; D_i is the distance from the center of block i to the common interface of blocks i and j; and $k_{ij+1/2}$ is an averaged (such as harmonic-weighted) absolute permeability along the connection between elements i and j. The flow potential term in Equation (19) is defined as,

$$\Phi_{\beta i} = P_{\beta i} - \rho_{\beta,ij+1/2}\, g\, Z_i \tag{22}$$

where Z_i is the depth to the center of block i from a reference datum.

Handling Klinkenberg effect: To include the Klinkenberg effect on gas flow, the absolute permeability to gas phase in Equation (21) should be evaluated using Equation (11) as a function of gas phase pressure.

Handling "non-Newtonian" flow: In the case that gas or water flow is subject to a threshold potential gradient, the discrete potential gradient in Equation (19) should be replaced by the effective potential gradient, Equation (14), for phase flow term evaluation.

Handling non-Darcy flow: Under the non-Darcy flow condition of Equation (12), the flow term ($\text{flow}_{\beta,ij}$) in Equation (19) along the connection (i, j), between elements i and j, is numerically defined as (Wu, 2002),

$$\text{flow}_{\beta,ij} = \frac{A_{ij}}{2\left(k\beta_\beta\right)_{ij+1/2}}\left\{-\frac{1}{\lambda_\beta} + \left[\left(\frac{1}{\lambda_\beta}\right)^2 - \bar{\gamma}_{ij}\left(\Phi_{\beta j} - \Phi_{\beta i}\right)\right]^{1/2}\right\} \tag{23}$$

in which the non-Darcy flow transmissivity is defined as,

$$\bar{\gamma}_{ij} = \frac{4\left(k^2\rho_\beta\beta_\beta\right)_{ij+1/2}}{D_i + D_j} \tag{24}$$

In evaluating the "flow" terms in the above Equations (19)-(24), subscript ij+1/2 is used to denote a proper averaging or weighting of fluid flow properties at the interface or along the connection between two blocks or nodes i and j. The convention for the signs of flow terms is that flow from node j into node i is defined as "+" (positive) in calculating the flow terms.

Equation (18) presents a precise form of the balance equation for each mass component of gas and water in a discrete form. It states that the rate of change in mass accumulation (plus adsorption or desorption, if existing) at a node over a time step is exactly balanced by inflow/outflow of mass and also by sink/source terms, when existing for the node. As long as all flow terms have the flow from node i to node j equal to and opposite to that of node j to node i for fluids, no mass will be lost or created in the formulation during the solution. Therefore, the discretization in Equation (18) is conservative.

Handling fractured media: Handling flow through fractured media is critical in shale gas reservoir simulation, because gas production from such low-permeability formations relies on fractures, from hydraulic fractures/network to various scaled natural fractures, to provide flow channels for gas flow into producing wells. Therefore, any unconventional reservoir simulator must have the capability of handling fractured media. The published modeling exercises in the literature have paid a lot of attention to modeling fractures in shale gas formations (e.g., Cipolla, 2009; Freeman et al. 2009a; 2009b; 2010; Moridis et al. 2010; Cipolla et al. 2010; Rubin, 2010; Li et al. 2011; Wu et al. 2012). However, it should be pointed out that there have been very few studies carried out to address the critical issues how to accurately simulate fractured unconventional gas reservoirs or to select the best approach for modeling a given shale gas formation. Most of the modeling exercises use commercial reservoir simulators, developed for conventional fractured reservoir simulation, which have very limited capabilities of modeling multi-scaled or complicated fractured reservoirs. On the other hand, in order to simulate fractured unconventional gas reservoirs, more efforts on model developments are needed from new conceptual models to in-depth modeling studies of laboratory to field scale application.

In our opinion, the hybrid-fracture modeling approach, defined as a combination of explicit-fracture (discrete fracture model), MINC (Pruess and Narasimham, 1985), and single-porosity modeling approaches, seems the best option for modeling a shale gas reservoir with both hydraulic fractures and natural fractures. This is because hydraulic fractures, which have to be dealt with for shale gas production, are better handled by the explicit fracture method, and they cannot be modeled in general by a dual-continuum model. On the other hand, natural fractured reservoirs are better modeled by a dual-continuum approach, such as MINC for extremely low-permeability matrix in shale gas formations, which cannot be modeled by an explicit fracture model.

Explicit fracture or discrete fracture concept is explicitly to include every fracture in the modeled system using refined grids to discretize fractures and the matrix surrounding fractures. This approach is a good option for simulating hydraulic fractures for gas production from hydraulic fractured wells in a non-fractured shale gas reservoir. The advantage of this approach is that it can model hydraulic fractures accurately when the fractures are known for their spatial distributions, determined from other fracture characterization studies. The disadvantage is that it cannot be used for simulating natural fractures or micro fractures in general, because the number of natural or micro fractures in a shale gas reservoir is too large for the model to handle.

For the low matrix permeability or large matrix block size, the traditional double-porosity model may not be applicable for modeling natural fractures in unconventional reservoirs. This is because it takes years to reach the pseudo-steady state under which the double-porosity model applies. The MINC concept (Pruess and Narasimham, 1985) is able to describe gradients of pressures, temperatures, or concentrations near matrix surface and inside the matrix–by further subdividing individual matrix blocks with one- or multidimensional strings of nested meshes, as shown in **Figure 4**. Therefore, the MINC method treats interporosity flow in a fully transient manner by computing the gradients which drive interporosity flow at the matrix-fracture interface. In comparison with the double-porosity or dual-permeability model, MINC does not rely on the pseudo-steady state assumption to calculate fracture-matrix flow and is able to simulate fully transient fracture-matrix interaction by subdividing nested-cell gridding inside matrix blocks. The MINC concept should be generally applicable for handling fracture-matrix flow in fractured shale gas reservoirs, no matter how large the matrix block size is or how low the matrix permeability is and is more suitable for handling fractured shale gas reservoirs. However, the MINC approach may not be applicable to systems in which fracturing is so sparse that the fractures cannot be approximated as a continuum.

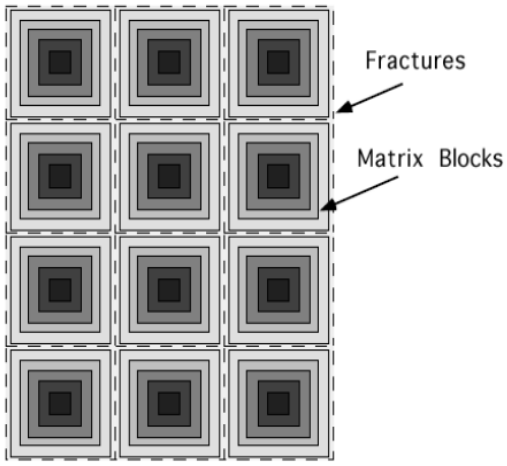

Figure 4 Schematic of MINC (multiple interacting continua) Concept (Pruess and Narasimham, 1985)

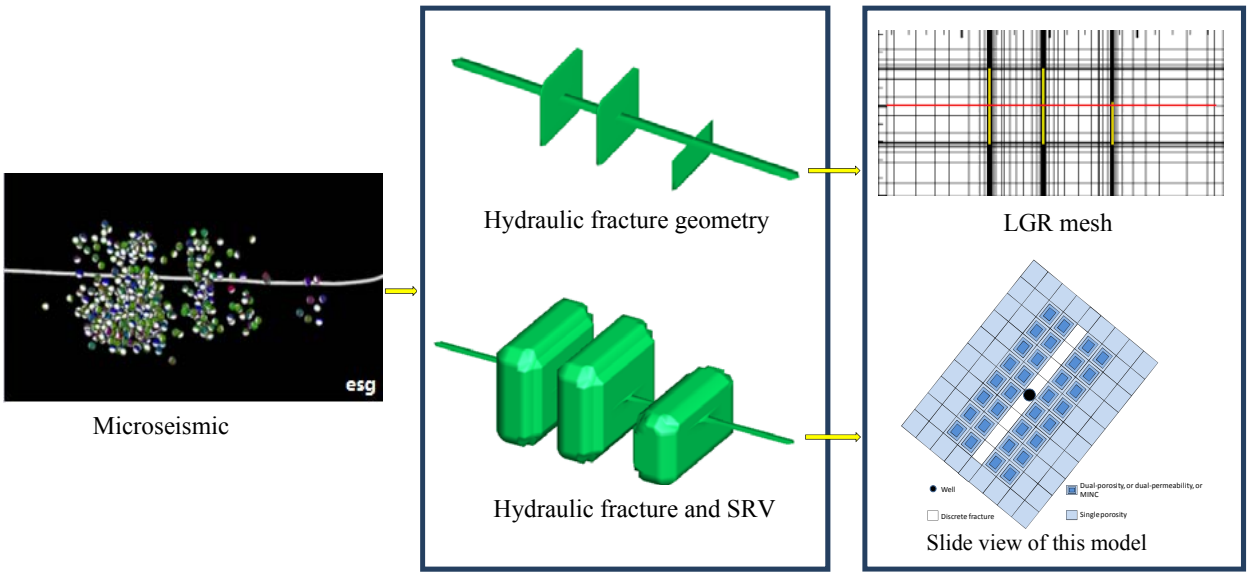

Figure 5 Hybrid-fracture model built methodology from microseismic cloud

As **Figure 5** shows, in our hybrid-fracture model, both the hydraulic fractures and stimulated reservoir volume (SRV) are evaluated from the microseismic cloud. Recent advances in microseismic fracture mapping technology have provided previously unavailable information to characterize hydraulic fracture growth, stimulated reservoir volume and have documented surprising complexities in many geological environments. We will have a primary hydraulic fracture system and an associated stimulated volume in each hydraulic fracture stage. First we define a primary fracture based on the orientation and region of the microseismic cloud. The hydraulic fractures are modeled by discrete fracture method. We assume the stimulated reservoir volume (SRV) near the hydraulic fractures is the area with natural fractures and we apply MINC in this area. Single-porosity is applied in the region outside the SRV. Local grid refinement (LGR) is used to improve simulation accuracy as pressure gradients change substantially over short distances in the regions near hydraulic fractures. LGR is performed near the hydraulic fracture region.

Numerical solution: In this work, we use the fully implicit scheme to solve the discrete nonlinear Equation (18) with a

Newton iteration method. Let us write the discrete nonlinear equation, Equation (18), in a residual form as,

$$R_i^{\beta,n+1} = \left\{ (\phi\rho S)_i^{\beta,n+1} + m_i^{\beta,n+1} - (\phi\rho S)_i^{\beta,n} - m_i^{\beta,n} \right\} \frac{V_i}{\Delta t} - \sum_{j\in\eta_i} flow_{ij}^{\beta,n+1} - Q_i^{\beta,n+1} = 0 \tag{25}$$

$$(\beta = 1, 2\,;\ i = 1, 2, 3, \ldots, N).$$

Equation (25) defines a set of 2×N coupled nonlinear equations that need to be solved for every balance equation of mass components, respectively. In general, two primary variables per node are needed to use the Newton iteration for the associated two equations per node. The primary variables selected are gas pressure and gas saturation. The rest of the dependent variables, such as relative permeability, capillary pressures, viscosity and densities, adsorption term, as well as nonselected pressure and saturation,—are treated as secondary variables, which are calculated from selected primary variables.

In terms of the primary variables, the residual equation, Equation (25), at a node i is regarded as a function of the primary variables at not only node i, but also at all its direct neighboring nodes j. The Newton iteration scheme gives rise to

$$\sum_m \frac{\partial R_i^{\beta,n+1}(x_{m,p})}{\partial x_m} (\delta x_{m,p+1}) = -R_i^{\beta,n+1}(x_{m,p}) \tag{26}$$

where x_m is the primary variable m with m = 1 and 2, respectively, at node i and all its direct neighbors; p is the iteration level; and i =1, 2, 3, …, N. The primary variables in Equation (25) need to be updated after each iteration,

$$x_{m,p+1} = x_{m,p} + \delta x_{m,p+1} \tag{27}$$

The Newton iteration process continues until the residuals $R_i^{\beta,n+1}$ or changes in the primary variables $\delta x_{m,p+1}$ over iteration are reduced below preset convergence tolerances.

Numerical methods are generally used to construct the Jacobian matrix for Equation (26), as outlined in Forsyth et al. (1995). At each Newton iteration, Equation (26) represents a system of (2×N) linearized algebraic equations with sparse matrices, which are solved by a linear equation solver.

Numerical Model Verification

To examine the accuracy of our simulator formulation in simulating porous medium gas flow with the Klinkenberg, non-Darcy flow, gas adsorption and geomechanics effect, several relevant steady and transient analytical solutions are derived or used for considering these flow mechanisms. The problem concerns steady-state and transient gas flow across a 1-D reservoir. The system contains steady/transient-state gas flow at an isothermal condition and a constant gas mass injection/production rate is imposed at one side of the rock or well. The other boundary of the rock/reservoir is kept at constant pressure. Eventually, the system will reach steady state, if the production is maintained for a long period of time. A comparison of the pressure profiles along the rock block from the simulation and the analytical solution is shown in **Figures 6 and 7,** indicating that our simulated pressure distribution is in excellent agreement with the analytical solutions for all the problems of 1-D linear flow with Klinkenberg or non-Darcy flow effect.

Details about the analytical solution derivation considering Klinkenberg and non-Darcy flow effect are included in our previous work (Wu et al. 2012) and we will show their verification results only in this section for 1-D linear flow steady flow situation. Comparisons between analytical and numerical solution for the radial flow and transient flow cases are also presented in our former work. Constant coefficients for Klinkenberg effect and correlation (13) for the non-Darcy flow coefficient are used with comparison results shown in **Figures 6 and 7**.

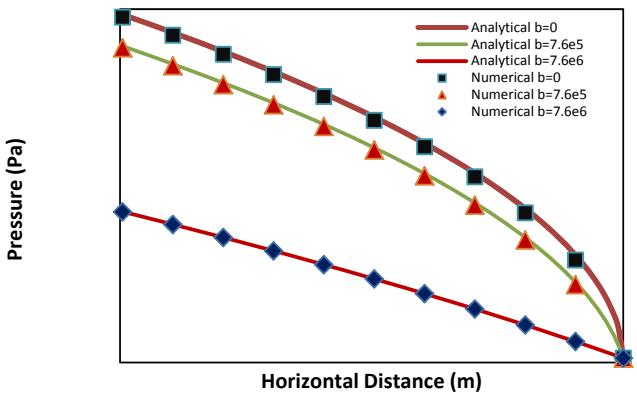

Figure 6 Analytical and Numerical Results for Linear s Flow with Klinkenberg Effect

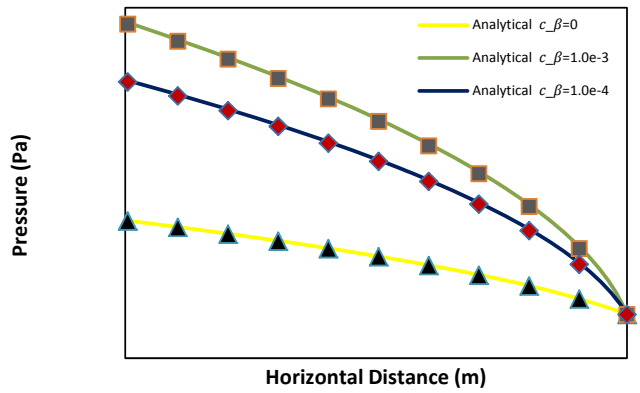

Figure 7 Analytical and Numerical Results for Linear non-Darcy Flow

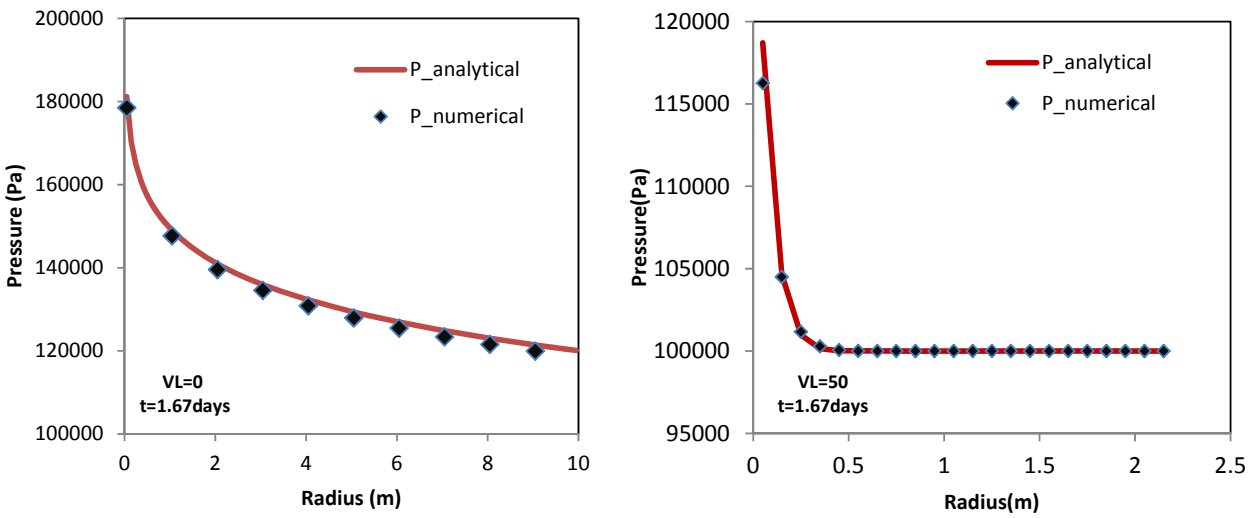

Figure 8 Comparison of gas pressure profiles considering gas adsorption in a radial system at 1.67 days, calculated using the numerical and analytical solutions

Verification for flow with adsorption: For the gas flow with adsorption, the analytical solution is given in Appendix A. The parameters used for this comparison study are: porosity $\Phi = 0.15$; $\Phi = 0.15\Phi = 0.15$; permeability k = 100 mD; k = 100 md; k = 100 md; formation temperature $T = 25^{o}C$; $T = 25^{o}C$; gas viscosity $\mu = 1.64 \times 10^{-2}$cp; $\mu = 1.64 \times 10^{-2}$cp ; initial pressure $P_i = 10^5$Pa; $P_i = 10^5$Pa and thickness of the radial system is 1m. The well boundary condition is: air mass injection rate: $Q = 1.0 \times 10^{-4}$kg/s; $Q = 1.0 \times 10^{-4}$kg/s.

Figure 8 presents the comparisons of the pressure profile at 1.16 days from the numerical and analytical solutions. Two situations, Langmuir volume $V_L = 0$; $V_L = 0$ and $V_L = 50\ m^3/kg$; $V_L = 50\ m^3/kg$, are considered. The analytical solutions give excellent match with numerical solution.

Verification for linear flow with geomechanics: Wu and Pruess (2000) presented an analytical method for analyzing the non-linear coupled rock permeability variation and fluid flow problem. Approximate analytical solutions for one-dimensional linear and radial flow are obtained by an integral method, which is widely used in the study of steady and unsteady heat conduction problems. The accuracy of integral solutions is generally acceptable for engineering applications. When applied to fluid flow problems in porous media, the integral method consists of assuming a pressure profile in the pressure-disturbance zone and determining the coefficients of the profile by making use of the integral mass balance equation.

Table 1 Parameters for checking integral solution for flow with geomechanics effect

Parameter	Value	Unit
Initial pressure	$P_i = 10^7$	Pa
Initial porosity	$\Phi_i = 0.20$	
Initial fluid density	$\rho_w = 975.9$	kg/m^3
Cross-section area	A=1.0	m^2
Formation thickness	h=1.0	m
Fluid viscosity	$\mu = 0.35132 \times 10^{-3}$	$Pa \cdot s$
Fluid compressibility	$C_f = 4.556 \times 10^{-10}$	Pa^{-1}
Rock compressibility	$C_r = 5.0 \times 10^{-9}$	Pa^{-1}
Initial permeability	$k_0 = 9.860 \times 10^{-13}$	m^2
Water injection rate	$q_m = 0.01$	kg/s
Hydraulic radius	$r_w = 0.1$	m
Exponential index	c=2.22	

The parameters as shown in Table 1 are used to evaluate both the numerical solution and the integral solution. A comparison of injection and the exact numerical solutions is shown in **Figure 9**. The agreement between the two solutions is excellent for the entire transient period.

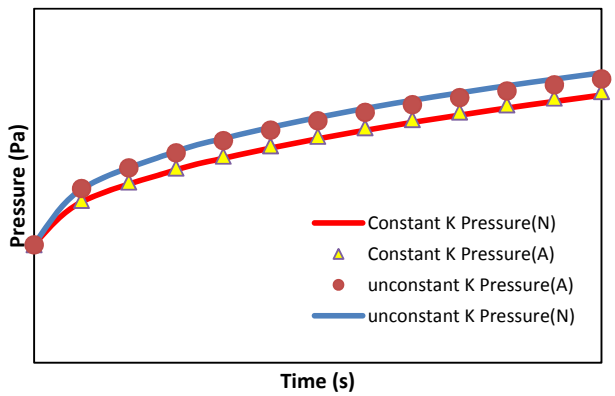

Figure 9 Comparison of injection pressures calculated from integral and numerical solutions for linear flow in a permeability-dependent medium with constant and unconstant permeability function

Model Application

In the following model application examples, we are concerned with gas flow towards one horizontal well and 10-staged hydraulic fracture system in an extremely tight, uniformly porous and/or fractured reservoir **(Figure 10)**. The reservoir formation is at liquid-gas, two-phase condition, however, the liquid saturation is set at residual values as an immobile phase. This is a single-phase gas flow problem and is modeled by the two phase flow reservoir simulator. The immobile liquid flow is controlled by liquid relative permeability curves.

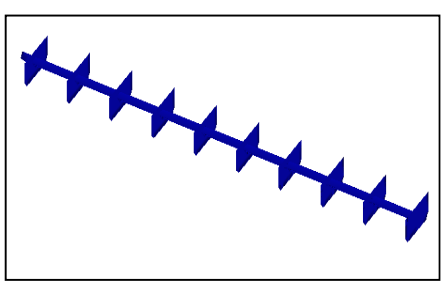

Figure 10 Horizontal and multi-staged hydraulic fracture model

We demonstrate the application of the proposed mathematical model for modeling gas production from a producer with 10-staged hydraulic fracturing in a shale gas reservoir. The stress alteration induced by hydraulic fracturing may activate existing natural fractures, and therefore opens microflow channels in the drainage area of the stimulated well. Here we present the simulation of a hydraulic fracturing problem as an example case to illustrate the capability of our hybrid fracture model to capture such complex fracture network in these reservoirs. Three different fracture models are built and their flow behavior is compared. The first one considers that there is no natural fractured-active area and the whole formation is single porosity shales with low permeability. In the second model, we assume that only the natural fractures within the stimulated reservoir volume (SRV) near the hydraulic fractures are active and the rest natural fractures outside the SRV remain inactive. An increase in pore pressure around the hydraulic fracture causes significant reduction in the effective stresses, potentially reopening the existing healed natural fractures or creating new fractures. As a result, the permeability near the well of the reservoir is significantly improved. This effect would help increase the well productivity in the initial production. The third fracture model is that all the formation is naturally fractured.

To simulate the performance of this system using our model, hydraulic fractures are represented by the discrete fracture model, an active naturally-fractured reservoir area is described by the mutli-continuum fracture model, while a non-active natural fractured reservoir area is represented by the single-porosity model. The basic parameter set for the simulation and discussion is summarized in **Table 2,** which are chosen field data.

We first compare the gas production behavior for these three fracture model. Then, based on the second fracture model, i.e., reactivated natural fractures only in SRV, we analysis the gas production curves with Klinkenberg, geomechanics and adsorption/desorption effects.

Table 2 Data used for the case studies

Reservoir length, Δx, ft	5500	Hydraulic fracture porosity, Φ_{hf}	0.5
Reservoir width, Δy, ft	2000	Hydraulic fracture total compressibility, c_{hf}, psi^{-1}	2.5E-04
Formation thickness, Δz, ft	250	Initial reservoir pressure, P_i, psi	3800
Horizontal well length, L_h, ft	4800	Constant flowing bottomhole pressure, P_{wf}, psi	500
Hydraulic fracture number	10	Reservoir temperature, T, ^oF,	200
Distance between hydraulic fractures, $2y_e$, ft	500	Klinkenberg coefficient, psi	200
Hydraulic fracture half-length, X_f, ft	250	Non-Darcy flow constant, c_β, $m^{3/2}$	3.2E-06
Viscosity, μ, cp	0.0184	Langmuir's pressure, P_L, psi	2285.7
Matrix permeability, k_m, md	1.6E-02	Langmuir's volume, V_L, scf/ton	218.57
Matrix porosity, Φ_m	0.05	Natural fracture total compressibility, c_{nf}, psi^{-1}	2.5E-04
Matrix total compressibility, c_{tm}, psi^{-1}	2.5E-04	Hydraulic fracture permeability, k_{hf}, md	1E05
Natural fracture permeability, k_{nf}, md	1000	Reservoir depth, h, ft	5800
Natural fracture porosity, Φ_{nf}	0.4		

Figure 11 compares the performance of the fractured horizontal well for the three fracture reservoirs. The comparison indicates that fracture model make a difference in well performance. The contribution from active natural fractures is evident and helps to yield higher production rates for a long period. Larger stimulated reservoir volume leads to higher a gas production rate.

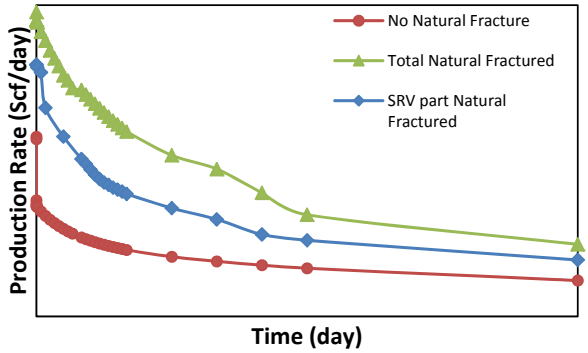

Figure 11 Simulated gas production performance for the three fracture models

For the second fracture model, pressure distribution at 1 year and 20 years are presented in **Figure 12** and **Figure 13**.

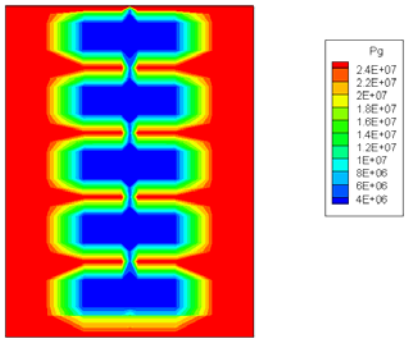

Figure 12 Pressure distribution at 1 year of fracture model#2

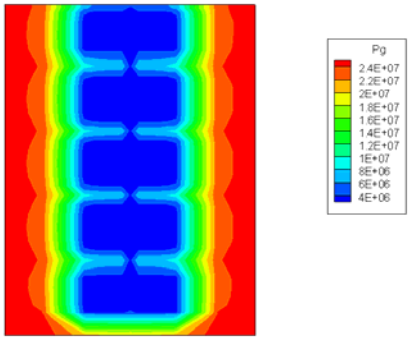

Figure 13 Pressure distribution at 20 years of fracture model#2

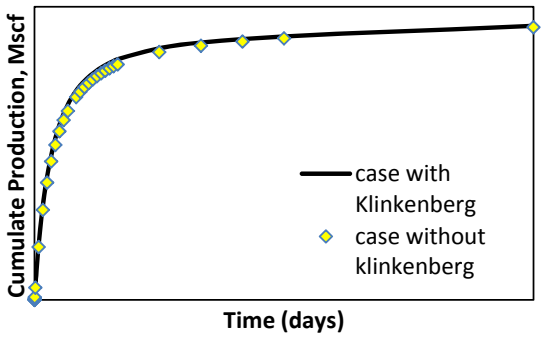

Figure 14 Gas cumulative production behavior with Klinkenberg effect

Figure 14 shows the simulated well cumulative production versus time with and without Klinkenberg effect. It is interesting to note that Klinkenberg effect just causes small increase for the matrix permeability in this case. Because the matrix permeability is so small compared with natural fracture or hydraulic fracture permeability, this small change has little influence on the total production rate.

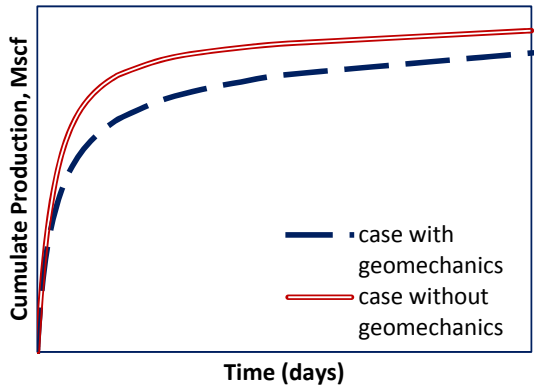

Figure 15 Gas cumulative production behaviors with geomechanics

Figure 15 shows the simulated well cumulative production versus time with and without geomechanics effect. The relationship used for describing effective stress and permeability of the unconventional reservoir is shown in **Figure 2**. As sown in **Figure 15**, geomechanics-flow coupling has large impact on formation permeability especially for the natural fracture system. Take the Muska formation for example, when the effective stress increase from 1,600 psia to 4,800 psia, permeability decreases to 1/20 of its original value. With the gas production, reservoir effective stress increases as pore pressure decreases, leading to the reduction of cumulative gas production.

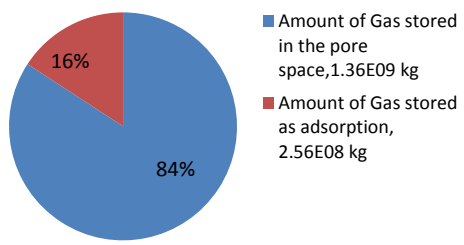

Figure 16 Adsorbed gas and free gas amount at initial condition

Figures 16, 17 and **18** present the results for adsorption analysis using the numerical model. Based on the data in **Table 2**, we calculate the total gas mass as free gas in the micropores and adsorbed gas on surface at initial condition. Then we compare the cumulative gas production with and without considering adsorption. Simulation results (**Figure 17**) show the estimated gas production will increase with considering adsorption. This difference will become more and more evident. For the situation considering gas adsorption/desorption, gas production from the adsorption is about 13% and the produced portion of the free gas consists of 87%, as shown in **Figure 18**.

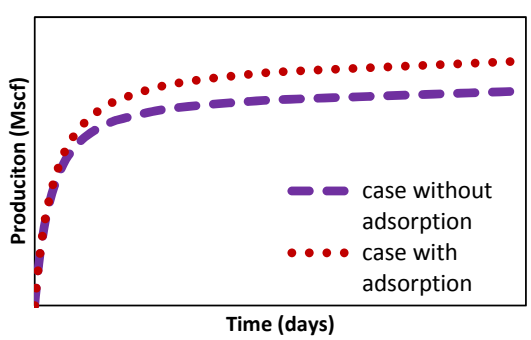

Figure 17 Gas cumulative production behaviors with adsorption

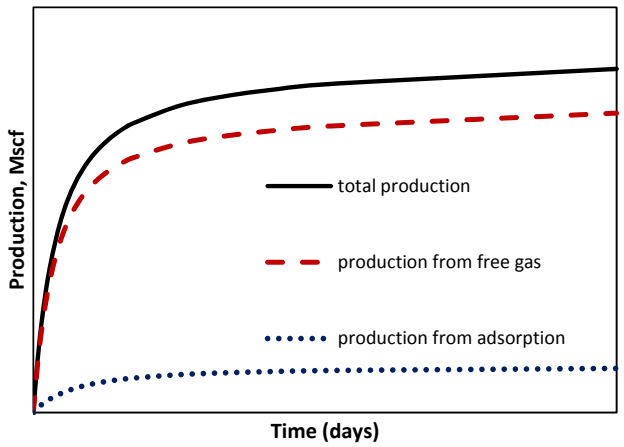

Figure 18 Gas production component analysis from adsorpted gas and free gas

Summary and Conclusions

This paper discusses a generalized framework mathematical model for modeling gas production from unconventional gas reservoirs. The model formulation incorporates known nonlinear flow processes, associated with gas production from low-permeability unconventional reservoirs, including Klinkenberg, non-Darcy flow, and nonlinear adsorption effects. The model formulation and numerical scheme are based on a generalized two-phase gas and liquid flow model using unstructured grids. Specifically, a hybrid modeling approach is presented by combining discrete fracture, multi-domain, and multi-continuum concepts for handling hydraulic fractures and fracture network in simulated reservoir volume (SRV), distributed naturally fractures, microfractures as well as porous matrix. We have verified the numerical models against analytical solutions for Klinkenberg, non-Darcy flow, and nonlinear adsorption effects.

As application examples, we present modeling studies using three-type fracture models for gas production from a ten-staged hydraulic fractured horizontal well, incorporating Klinkenberg effect, non-Darcy flow and nonlinear adsorption effects. The model results show there is a large impact of various fracture models on gas production rates as well as cumulative production.

Acknowledgments

This work was supported in part by EMG Research Center and UNGI of Petroleum Engineering Department at Colorado School of Mines; by Foundation CMG; by RIPED of PetroChina Co.; and by IFPEN.

References

Blasingame, T.A., “The Characteristic Flow Behavior of Low-Permeability Reservoir Systems,” SPE 114168, presented at the 2008 SPE Unconventional Reservoirs Conference held in Keystone, Colorado, U.S.A., 10–12 February 2008.

Bustin, R.M., A.M.M. Bustin, X. Cui, D.J K Ross, and V.S. Murthy Pathi, “Impact of Shale Properties on Pore Structure and Storage Characteristics,” SPE 119892, presented at the SPE Gas Production Conference, 16-18 November, Fort Worth, Texas, 2008.

Cipolla, C.L., N.R. Warpinski, M.J. Mayerhofer, E.P. Lolon, and M.C. Vincent, "The Relationship Between Fracture Complexity, Reservoir Properties, and Fracture Treatment Design," SPE 115769 presented at the SPE ATC&E, Denver, Colorado, U.S.A., 2009.

Cipolla, C.L., E.P. Lolon, J.C. Erdle, and B. Rubin, “Reservoir Modeling in Shale-Gas Reservoirs,” *Reservoir Evaluation & Engineering*, August 2010.

Cipolla, C.L., “Modeling Production and Evaluating Fracture Performance in Unconventional Gas Reservoirs,” *JPT*, Distinguished Author Series, pp.84-90, September 2009.

Davies, J.P. and D.K. Davies, “Stress-Dependent Permeability Characterization and Modeling,” SPE 56813, presented at SPE ATCE, Houston, TX, October 1999.

EIA (U.S. Energy Information Administration), World Shale Gas Resources: An Initial Assessment of 14 Regions Outside the United States, April 2011.

Forsyth, P. A., Y. S. Wu and K. Pruess, Robust Numerical Methods for Saturated-unsaturated Flow with Dry Initial Conditions in Heterogeneous Media. Advance in Water Resources 18, p. 25-38, 1995.

Freeman, C.M., G.J. Moridis, D. Ilk, D. and T.A. Blasingame, "A Numerical Study of Transport and Storage Effects for Tight Gas and Shale Gas Reservoir Systems," SPE 131583, presented at the SPE International Oil & Gas Conference and Exhibition held in Beijing, China, 8-10 June 2010.

Freeman, C.M., G.J. Moridis, and T.A. Blasingame, "A Numerical Study of Microscale Flow Behavior in Tight Gas and Shale Gas Reservoir Systems," Proceedings, 2010 TOUGH Symposium, Berkeley, CA, 14-16 September, 2009a.

Freeman, C.M., G.J. Moridis, D. Ilk, , and T.A. Blasingame, "A Numerical Study of Tight Gas And Shale Gas Reservoir Systems," SPE 124961, presented at the SPE Annual Technical Conference and Exhibition, New Orleans, Louisiana, 4-9 October, 2009b.

Gao, C., J.W. Lee, J.P., Spivey, and M.E. Semmelbeck, "Modeling Multilayer Gas Reservoirs Including Sorption Effects," SPE 29173, presented at the SPE Eastern Regional Conference & Exhibition, Charleston, West Virginia, 8-10 November 1994.

Kelkar M. and M. Atiq, "Upgrading Method for Tight Gas Reservoirs," SPE 133301, presented at the SPE Annual Technical Conference and Exhibition, Florence, Italy, 19-22 September, 2010.

Klinkenberg, L.J., "The Permeability of Porous Media to Liquids and Gases," in API Drilling and Production Practice, 200–213, 1941.

Langmuir, I., "The constitution and fundamental properties of solids and liquids," *Journal of the American Chemical Society*, 38 (11): 2221–2295, 1916.

Leahy-Dios, Alana, Mlta Das, Anshul Agarwal, Robert D. Kaminsky, "Modeling of Transport Phenomena and Multicomponent Sorption for Shale Gas and Coalbed Methane in an Unstructured Grid Simulator", SPE 147352, presented at the SPE Annual Technical Conference, Denver, Colorado, 30 Octomber-2 November 2011

Lei, Qin, Wei Xiong, Jiangru Yuan, Yuquan Cui, and Yu-Shu Wu, Analysis of Stress Sensitivity and Its Influence on Oil Production from Tight Reservoirs, SPE-111148, presented at the 2007 SPE Eastern Regional Meeting held in Lexington, Kentucky, U.S.A., 17–19 October 2007.

Leverett, M.C., "Capillary Behavior in Porous Media," *Trans* AIME, 142:341-358, 1941.

Li, J., C.M, Du, and X. Zhang, "Critical Evaluation of Shale Gas Reservoir Simulation Approaches: Single-Porosity and Dual-Porosity Modeling," presented at the SPE Middle East Unconventional gas Conference and Exhibition, Muscal, Oman, 31 January–2 February 2011.

Mengal, S.A. and R.A. Wattenbarger, "Accounting For Adsorbed Gas in Shale Gas Reservoirs," SPE 141085, presented at the SPE Middle East Oil and Gas Show and Conference held in Manama, Bahrain, 25–28 September 2011.

Moridis, G.J., T.A. Blasingame, and C.M. Freeman, "Analysis of Mechanisms of Flow in Fractured Tight-Gas and Shale-Gas Reservoirs," SPE 139250, presented at the SPE Latin American & Caribbean Petroleum Engineering Conference held in Lima, Peru, 1–3 December 2010.

Pruess, K., C. Oldenburg and G. Moridis, *TOUGH2 User's Guide, Version 2.0,* Report LBNL-43134, Berkeley, California: Lawrence Berkeley National Laboratory, 1999.

Pruess, K. and T.N. Narasimhan, "A Practical Method for Modeling Fluid And Heat Flow in Fractured Porous Media," *Soc. Pet. Eng. J.,* 25, 14-26, 1985.

Pruess, K., GMINC-A mesh generator for flow simulations in fractured reservoirs, Report LBL- 15227, Berkeley, California: Lawrence Berkeley National Laboratory, 1983.

Rubin, B., "Accurate Simulation of Non-Darcy Flow in Stimulated Fractured Shale Reservoirs," SPE 132093, presented at the SPE Western Regional Meeting held in Anaheim, California, USA, 27–29 May 2010.

Rutqvist, J. Y.S. Wu, C.F. Tsang, and G.S. Bodvarsson, "A Modeling Approach for Analysis of Coupled Multiphase Fluid Flow, Heat Transfer, and Deformation in Fractured Porous Rock," *International Journal of Rock Mechanics and Mining Sciences,* Vol. 39, 429-442, 2002.

Silin, D. and T. Kneafsey, "Gas Shale: From Nanometer-scale Observations to Well Modeling," CSUG/SPE 149489, presented at the Canadian Unconventional Resources Conference, Calgary, Alberta, Canada, 15-17 November, 2011.

Soeder, D.J., "Porosity and Permeability of Eastern Devonian Gas Shale," *SPE Formation Evaluation*, pp. 116-124, March 1988.

Tek, M.R., Coats, K.H., Katz, D.L., "The Effects of Turbulence on Flow of Natural Gas through Porous Reservoirs," *J. Pet. Technol. Trans*. AIME 222, 799–806, 1962.

Wang, F.P., R.M. Reed, J.A. Jackson, and K.G. Jackson, "Pore Networks and Fluid Flow in Gas Shales," SPE 124253, presented at the 2009 SPE Annual Technical Conference and Exhibition held in New Orleans, Louisiana, USA, 4–7 October 2009.

Winterfeld, P. H. and Y.S. Wu, "A Novel Fully Coupled Geomechanical Model for CO2 Sequestration in Fractured and Porous Brine Aquifers," presented at the XIX International Conference on Water Resources CMWR 2012, University of Illinois at Urbana-Champagne June 17-22, 2012.

Winterfeld, P. H. and Y.S. Wu, "Parallel Simulation of CO2 Sequestration with Rock Deformation in Saline Aquifers," SPE 141514, prepared for presentation at the SPE Reservoir Simulation Symposium held in The Woodlands, Texas, USA, 21–23 February 2011.

Wu, Y.S. and C. Wang, "Transient Pressure Testing Analysis of Gas Wells in Unconventional Reservoirs," SPE-SAS-312, presented at the 2012 SPE Annual Technical Symposium & Exhibition (ATS&E), Khobar, Saudi Arabia, 8-11 April 2012.

Wu, Y.S., C, Wang, J. Li, and P. Fackahroenphol, "Transient Gas Flow in Unconventional Gas Reservoirs," SPE-154448, presented at the EAGE Annual Conference & Exhibition incorporating SPE Europec held in Copenhagen, Denmark, 4–7 June 2012.

Wu, Y.S., J. Rutqvist, K. Karasaki, Q. Lei, W. Xiong, J. Yuan, M. Liu, and Y. Di, A Mathematic Model for Rock Deformation Effect of Flow in Porous and Fractured Reservoirs," presented at the 42nd US Rock Mechanics Symposium and 2nd U.S.-Canada Rock Mechanics Symposium, San Francisco, CA, 2008.

Wu, Y.S., "Numerical Simulation of Single-Phase and Multiphase Non-Darcy Flow in Porous and Fractured Reservoirs,"

Wu, Y.S., K. Pruess "Intergral solutions for transient fluid flow through a porous medium with pressure-dependent permeability", *International Journal of Rock Mechanics and Mining Sciences,* 37, 51-61, 2000.

Wu, Y.S. and K. Pruess "A numerical method for simulating non-Newtonian fluid flow and displacement in porous media", Vol. 21, Advances in Water Resources, 351-362, 1998.

Wu, Y.S., K. Pruess, and P. Persoff, "Gas Flow in Porous Media with Klinkenberg Effects," *Transport in Porous Media*, Vol.32, 117-137, 1998.

Wu, Y.S., K. Pruess, and P.A. Witherspoon, "Flow and Displacement of Bingham Non Newtonian Fluids in Porous Media," *SPE Reservoir Engineering*, pp.369 376, 1992.

Xiong, Wei, Qun Lei, Jiangru Yuan, Shusheng Gao, and Yu-Shu Wu, "Behavior of Flow through Low-Permeability Reservoirs," SPE-113144, prepared for presentation at the 2008 SPE EUROPEC Conference to be held in Rome, Italy, 9-12 June 2008

Zhao, X., "An Experimental Study of Methane Diffusion in Coal Using Transient Approach," Ph.D. Dissertation, Department of Mining And Geological Engineering, The University of Arizona, 1991.

Appendix A

In this appendix, we derive the analytical solution for gas flow with adsorption/desorption. If the system is isothermal, the ideal gas law applies, and gravity effect is negligible, then gas flow in porous media with adsorption is described by the following equations,

$$\nabla \cdot (\rho v) = -\frac{\partial(\phi\rho + m_g)}{\partial t} \tag{A-1}$$

where ρρ is the gas density; v is the gas flow velocity; ϕ is the porous media porosity; m_g is the adsorbed gas mass in a unit formation volume at given pressure; and t is the time.

According to the ideal gas law,

$$PV = nRT \tag{A-2}$$

$$\rho = \frac{M}{RT}P = \beta P \tag{A-3}$$

where M is gas molecular weight; R is universe gas constant; and β is a coefficient, for simplicity, defined as $\beta = \frac{M}{RT}$; T is the system temperature.

From Darcy's Law and Langmuir isotherm (Equations (2) and (3)),

$$v = -\frac{k}{\mu}\nabla P \tag{A-4}$$

$$m_g = \rho_R \rho_g V_E = \rho_R \rho_g V_L \frac{P}{P + P_L} = V\alpha \frac{P}{P + P_L} \tag{A-5}$$

where ρ_R is rock bulk density; ρ_g is gas density at standard condition; V_E is the adsorption isotherm function for gas content; V_L is the Langmuir's volume in scf/ton; and P_L P_L is Langmuir's pressure. α is a coefficient, for simplicity, defined as $\alpha = \rho_R \rho_g V_L$

Substituting Equations (A-4) and (A-5) into Equation (A-1), we will have

$$\nabla \cdot \left(\beta \frac{k}{\mu} P \nabla P \right) = \phi\beta \frac{\partial P}{\partial t} + \alpha \frac{\partial \left(\frac{P}{P + P_L} \right)}{\partial t} \tag{A-6}$$

In the radial coordinate,

$$\frac{1}{r}\frac{\partial}{\partial r}\left(r \frac{\partial P^2}{\partial r} \right) = \frac{2\phi\mu}{k}\frac{\partial P}{\partial t} + \frac{2\alpha\mu}{\beta k}\frac{\partial \left(\frac{P}{P + P_L} \right)}{\partial P}\frac{\partial P}{\partial t} \tag{A-7}$$

$$\frac{1}{r}\frac{\partial}{\partial r}\left(r \frac{\partial P^2}{\partial r} \right) = \left[\frac{2\phi\mu}{k} + \frac{2\alpha\mu}{\beta k}\frac{P_L}{\left(P + P_L \right)^2} \right]\frac{\partial P}{\partial t} \tag{A-8}$$

$$\frac{1}{r}\frac{\partial}{\partial r}\left(r \frac{\partial P^2}{\partial r} \right) = \left[\frac{\phi\mu}{Pk} + \frac{\alpha\mu}{P\beta k}\frac{P_L}{\left(P + P_L \right)^2} \right]\frac{\partial P^2}{\partial t} \tag{A-9}$$

The equation becomes:

$$\frac{1}{r}\frac{\partial}{\partial r}\left(r \frac{\partial P^2}{\partial r} \right) = \frac{1}{A}\frac{\partial P^2}{\partial t} \tag{A-10}$$

where we define the coefficient,

$$\frac{1}{A} = \frac{\phi\mu}{\overline{P}k} + \frac{\alpha\mu}{\overline{P}\beta k}\frac{P_L}{\left(\overline{P} + P_L \right)^2} \tag{A-11}$$

We propose to use a history-dependent, constant, averaged pressure within the pressure changed domain (Wu et al. 1998),

$$\overline{P} \approx \frac{\sum V_j P_j}{\sum V_j} \tag{A-12}$$

where V_j is a controlled volume at the geometric center of which the pressure was P_j at the immediate previous time when the solution was calculated. The summation, $\sum V_j$, is done over all V_j where pressure increases (or decreases) occurred at the previous time value. P_j is always evaluated analytically at point j, based on the previous estimated, constant diffusivity.

The well boundary proposed as a line source/sink well:

$$\lim_{x\to 0}\frac{\pi khr\beta}{\mu}\frac{\partial P^2}{\partial r}=Q_m \tag{A-13}$$

Then, we could get transient pressure solution for gas flow with adsorption/desorption,

$$P^2(r,t)=P_i^2-\frac{\mu Q_m}{2\pi khr\beta}Ei(-\frac{r^2}{4At}) \tag{A-14}$$